AD

REPORT NO. 3

FACTORS IN THE DESIGN OF POROUS ELECTRODES FOR PRIMARY ELECTROCHEMICAL CELLS

L. G. Austin
E. G. Gagnon

Department of Materials Science
Fuel Science Section

MAY 1969

United States Army Materiel Command
Harry Diamond Laboratories
Washington, D. C. 20438

Prepared by

College of Earth and Mineral Sciences
Pennsylvania State University

Under

Contract No. DAAG39-67-C-0065

43

The findings in this report are not to be construed as an official Department of the Army position, unless so designated by other authorized documents.

Destroy this report when it is no longer needed. Do not return it to the originator.

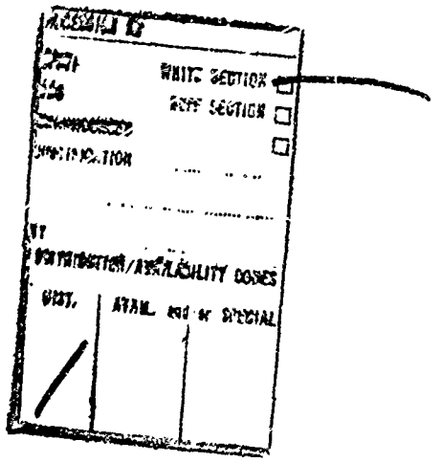

AD

DA-1T061102A34A
AMCMS Code: 5011.11.86000
HDL Proj: 96800

REPORT NO. 3

FACTORS IN THE DESIGN OF POROUS ELECTRODES FOR PRIMARY ELECTROCHEMICAL CELLS

L. G. Austin
E. G. Gagnon

Department of Materials Science
Fuel Science Section

MAY 1969

United States Army Materiel Command
Harry Diamond Laboratories
Washington, D. C. 20438

Prepared by

College of Earth and Mineral Sciences
Pennsylvania State University

Under

Contract No. DAAG39-67-C-0065

ABSTRACT

The purpose of this work was to apply the theories of porous electrode behavior to thin, porous electrodes used at low ambient temperatures, to show how performance is affected by the relevant factors involved. The system chosen for study was the Ag-Ag_2O electrode operating in the low-freezing eutectic of aqueous KOH as electrolyte. The report describes the complexity of the cathodic discharge curve; voltage varied with discharge time in 6 distinct regions. One of these regions, a plateau of almost constant potential was studied in detail. The current density-voltage-temperature relations for this region followed a Tafel equation, with an activation energy of exchange current of 14.5 kcals/mole. For this system an analytical solution was obtained for the equation of behavior. Results from this solution agreed reasonably well with experimental results. In addition, the theory was used to predict the distribution of reaction throughout the electrode and experimental results agreed well with predicted. It is shown how the theory can be used to predict optimum electrode thickness, and how porosity, internal area and electrolyte conductivity affect the result.

TABLE OF CONTENTS

INTRODUCTION

Although there have been several recent reviews (1,2,3) of the concepts involved in the mode of operation of porous electrodes, it is apparent that these concepts are not yet being employed to the full extent of their usefulness, in designing cell electrodes. There are several reasons for this. First, the available treatments are quite complex mathematically and little attempt has been made to make them easy to use in practice. Second, many real systems are considerably more complex than the simple models which have been mathematically formulated, and it might seem at first glance that the models would be of little use in the real system. There is a need for a manual which could be used by design engineers simply by finding a treatment appropriate to a particular system in which they are interested. Such a manual cannot be prepared at the moment because there are not enough case histories to illustrate the practical use of the equations of electrodes and, indeed, many important systems have not been properly treated theoretically.

It is likely that in the next few years there will be sufficient theoretical and practical work done to establish quantitative design criteria for all electrode systems of interest. The work described here is toward that end: it takes a particular electrode system and demonstrates the data which has to be found, and how complex general equations can be simplified to fit this particular system. As in most practical systems, a decision has to be made between the labor and expense of the work necessary for deeper and deeper understanding of the system, and the practical return from this more detailed understanding. This report illustrates this decision-making process for the particular system chosen.

No attempt will be made here to summarize the concepts involved in the formulation of quantitative theories of electrode behavior, and, it will be assumed that the reader is familiar with a standard treatment, that by Austin (2) for example. Simply stated, the objective of such a treatment is to describe the effect on electrode performance of parameters such as active surface area, porosity, electrode thickness, electrolyte conductivity, temperature, electroforming versus cold-pressing methods of preparation, etc. Eventually, it is the influence of these parameters on cell performance as a whole which is important, but it is clear that we need a description of each cell component before it is possible to solve the complete problem.

The electrode system chosen for study was the $Ag-Ag_2O/KOH(aq)$ electrode operating at low temperatures. This system was chosen because it is of interest in Zn-KOH silver oxide cells; because although it is quite a complex system yet it is simple enough to offer solution without excessive work; and because Harry Diamond Laboratories had quite a lot of experimental experience with the $Zn-KOH-Ag_2O$ cell at low temperatures.

LITERATURE AND BACKGROUND INFORMATION

It is well-known that the performance of Zn-KOH-silver oxide cells decreases considerably at temperatures less than 0°F. Our preliminary results on thin, porous electrodes (4) supplied by Harry Diamond Laboratories, Army Materiel Command, indicated that the major loss of performance was caused by increased polarization at the silver oxide electrode. It was decided, therefore, to perform a detailed half-cell study of the behavior of silver oxide electrodes in KOH eutectic (31 weight percent), concentrating at first on Ag-Ag_2O electrodes to avoid the complexity of mixed Ag_2O-AgO compositions during discharge.

Although the formation of Ag_2O and AgO on silver by anodic charging has been studied at room temperature (5,6) using a variety of electrochemical techniques, cathodic discharge at low temperatures has not been widely investigated. The form of the anodic charge of solid silver at constant current is well-known: polarization increases rapidly by double-layer charging until Ag_2O is formed on the surface, then polarization decreases somewha to a plateau. After some time, polarization increases from this plateau to the AgO formation potential, passes through a peak, and again decreases to a higher plateau corresponding to continued AgO formation from Ag_2O and Ag; polarization eventually increases to oxygen evolution. Since Ag_2O is poorly conductive, it was originally postulated (7) that the potential overshoot for the $Ag_2O \rightarrow AgO$ reaction was due to the ohmic resistance of a film of Ag_2O covering the silver surface. Once some AgO was formed, the ohmic polarization decreased due to the high conductivity of AgO. Other work (5,8) indicated that the potential overshoots are primarily nucleation polarizations and that the films of oxide formed are not sufficiently continuous to give high electronic ohmic resistance. Again, it was once postulated (9) that the inability to discharge AgO completely to Ag_2O near the expected potential (0.60 volts versus standard hydrogen) was due to hindrance of solid-state oxygen ion transfer through continuous oxide films. There is, however, good evidence (10) that thick, continuous films are not formed on anodic charge and that silver is removed from the surface and redeposited in the form of attached crystalites of Ag_2O, followed by disappearance of these crystals and the appearance of discrete AgO crystalites on the surface. Similarly, on discharge, massive rearrangement of the molecules occurs to give new crystal forms. The growth size of the crystalites is a function of rates of charge and discharge, being small at high current densities; lower current densities give fewer but larger crystalites.

The effect of porosity of practical battery electrodes can give added complexity to interpreting results. The reactions involve transfer of ions dissolved in the electrolyte contained in the pores of the electrode, and potential gradient is required for this transfer. This has the effect of making polarization greater at the exterior of the electrode (1,2,3). This effect is more pronounced for thicker electrodes, and it is possible during charge for potential in the

interior to correspond to the $Ag-Ag_2O$ reaction, and potential at the exterior to correspond to Ag_2O-AgO. These effects are enhanced at low temperatures: for example, the specific resistance of eutectic KOH goes from 1.9 ohm cm at 60°F to 33 ohm cm at -60°F.

In the experiments described below, particular attention was devoted to obtaining data on nucleation overshoots, electronic resistance effects, and the effect of porosity. In addition to the importance of low-temperature performance in some practical situations, operation at low temperature is interesting scientifically because it accentuates effects which may be only minor at room temperature conditions.

EXPERIMENTAL TECHNIQUES

A 250 mil beaker with a lucite cover was used as the electrochemical cell. The lucite cover contained five holes, three for the test, counter and reference electrodes, one for nitrogen gas used to deaerate the electrolyte, and one hole for a glass u-tube which was used to remove trapped gas bubbles that occasionally formed on the surface of the electrode during a run. The electrolyte was a 31 weight percent aqueous KOH solution, prepared from a 45 percent w/w Fischer reagent (Cat. No. SO-P-236) and distilled water that had been obtained from a Barnstead Still (Model No. SM-5). The temperature of the cell was controlled by a Tenney Jr. Test chamber (Model TJR) capable of controlling temperatures between -100°F to 350°F to within ± 1°F; electrical contacts were made through a terminal board on one of the walls of the chamber. The temperature within the chamber was measured with a chromel P-alumel thermocouple in conjunction with a Keithley DC Differential Voltmeter (Model 660).

The test electrodes had a plane surface area of 0.317 cm^2 and were obtained by using a punch and die, where the die opening was 0.25 in. The electrode discs were press fitted into a Teflon collar where the opening had been machined about 1 mil less than the diameter of the electrode disc. The Teflon collar containing the electrode was then screwed onto a Teflon shaft as shown in Figure 1; and the electrode pressed tightly against the current collector using the adjustable 1/4-inch rod shown, which was then removed. A platinum screen was used as a current collector, positioned between the electrode and the solid Teflon shaft. An external contact wire was connected to the screen and passed up through the center of the Teflon shaft. The electrode holder thus exposed one face of the electrode to the electrolyte and ensured uniform current density through this face. A coil of silver wire was used as counter electrode, and the surface of the wire was cleaned periodically of reaction products by dipping the wire into an HNO_3-distilled water solution (1:1) for several seconds and then throughly rinsing the electrode in distilled water.

A Hg/HgO/31 percent KOH reference electrode was used, and was prepared as described by Hamer and Craig (11). A salt bridge filled

with 31 percent KOH was placed between the test and reference electrodes. One end of the salt bridge ended in a fine capillary (Luggin capillary) which was positioned close to the surface of the test electrode.

The cell was assembled in the test chamber with the test electrode raised above the level of the electrolyte, and the test chamber set to the appropriate temperature. The test electrode was then lowered into the electrolyte. Steady-state, open-circuit voltages versus the Hg/HgO reference electrode were measured before steady-state and unsteady-state galvanostatic measurements, with a Fairchild Digital Multimeter (Model 7000). Constant current measurements were made using the rapid-switching circuit described by Austin and Almaula (12) in conjunction with a Nesco (Model JY120A-2) chart recorder. The desired current flowing through the cell was determined by the known voltage generated from a Harrison (6206B) DC power supply and the value of the precision resistor in the control circuit of the galvanostatic circuit. A Potter and Brumfield Hg-wetted contact relay (Type JMY-115-22) was used to eliminate switching transients.

A Tektronic Type RM564 storage oscilloscope (Type 3A3 Differential Amplifier and Type 2B67 Time Base) and Polaroid camera (Model C-12) were used to record voltage-time traces up to a few seconds. On initiation of a current, a vertical blanked-out portion of the trace showed the immediate establishment of an ohmic potential change, referred to hereafter as ir polarization. This polarization includes the resistance of the ionic current path in electrolyte between the face of the electrode and the Luggin tip, and electronic resistance in the current path through the test electrode, current collector and wire to the point of attachment of the lead from the potential measuring device (recorder or oscilloscope). During galvanostatic discharge, currents were interrupted and the decay of polarization versus time measured with the oscilloscope. The blanked-out parts of the trace on break and make of the current were again used to indicate ir polarization at that stage of the discharge.

TEST ELECTRODES

One of the electrodes (HDL) shown in Table 2 was prepared by Whittaker Corporation according to the procedures developed by the Harry Diamond Laboratories. The procedures as supplied by Harry Diamond Laboratories are as follows.

An Ag_2O-deionized water slurry was extruded onto an expanded metal screen (Exmet 5AG5-5/0), sintered, and anodically charged (using both faces of the electrode) in a 9-10 percent $NaHCO_3$ solution for 60 minutes at a current density of 0.125 amps/in^2. The electrode material was then:

1. discharged in $NaHCO_3$ solution at 0.125 amp/in^2 for 60 minutes,

2. rinsed in deionized water for 30 minutes,
3. allowed to drain for 30 minutes,
4. dried at 165°F in a recirculating type oven for 30 minutes,
5. charged in 5 percent KOH at 2.5 amps/in^2 for 20 seconds,
6. rinsed in deionzed water for 30 minutes,
7. allowed to drain for 30 minutes,
8. placed in a 160°F dry vacuum chamber for 4 hours,
9. stored in dry nitrogen gas.

It will be noted that this procedure may leave some silver carbonate and AgO on the electrode, although at room temperature the electrode rapidly comes to the Ag_2O/Ag potential on immersion in electrolyte. The electrode is about 70 percent porous and contains silver (apart from the screen) and Ag_2O in approximately equal weights.

In order to test whether certain of the results were due to the electrolytic formation of the HDL electrode, and to provide more flexibility in the variation of important electrode properties, a number of electrodes were prepared by us as follows. Ag_2O powder (Fischer reagent grade) was well mixed with an equal weight of Ag powder (Fischer reagent grade) in a mechanical shaker. Some of this material was used to fabricate electrodes, while another part was mixed with minus 400 mesh $NaNO_3$ to give a mixture containing 35 weight percent of the salt. Electrodes were manufactured using the work of Morrell and Smith (13) as a starting point.

Silver expanded metal screen was etched in concentrated nitric acid for 30 seconds and well rinsed in distilled water. This roughened the surface and promoted adhension between powder and screen. A 0.25 inch diameter die of hardened steel was fitted with a bottom punch also of hardened steel, and a layer of the powder spread evenly on the face of the punch. A 0.25 inch diameter portion of screen was cut from the roughened screen with a paper punch, and placed on the surface of the powder. This was covered with another layer of powder, a top punch placed in the die, and the whole cold-compressed at 55,700 psi for 2 minutes. The electrode prepared in this way without $NaNO_3$ filler was about 20 percent porous and was mechanically strong. When the filler was present, the electrode was placed in 200 ml of distilled water and left for three days, with water replacement every day; the filler dissolved and slowly diffused out without mechanical rupture of the electrode structure. The electrode was then washed, and dried in a dessicator. This procedure gave an electrode of about 63 to 66 percent porosity. Similarly, an electrode of 80 percent porosity was prepared using 60 percent $NaNO_3$ and a pressure of 65,000 psi.

In an attempt to make electrodes containing high internal silver area, electrodes were made from Ag powder prepared by thermal decomposition of silver oxalate following the procedure of Schroeder et.al. (14). However, BET measurements on this powder showed it had areas of only 0.45 m^2/g instead of the 5 m^2/g expected.

RESULTS

It was found that the test electrodes reached a stable, open-circuit potential after a few minutes of immersion in the electrolyte at room temperature but took longer times at lower temperatures; for example, stabilization times were up to one hour at -70°F. The open-circuit potential was always within ± 10 mv of the expected theoretical value. Figure 2 shows the variation of the effective resistance (times three) obtained from the initial blanked-out portion of the oscilloscope trace as a function of temperature, for an undisturbed position of the Luggin capillary. Also shown is the specific resistance of the electrolyte (solid line). The two sets of results are in reasonable agreement at the various temperatures, indicating that the resistance is primarily due to the mean electrolyte path between the electrode and the tip of the Luggin capillary. This mean path length can be calculated from $r = \rho\ell/A$, r being measured resistance, ρ specific resistance, ℓ path length and A the plane area of the electrode; thus ℓ is approximately 1/9 cm, which appears to be reasonable from the dimensions and position of the Luggin capillary. The data at -52°F shows typical spread of results of repositioning the Luggin. There were sometimes differences between the effective resistances determined initially and at some later stage in discharge, but these differences were usually small, except as noted later.

Figure 3 shows typical results of polarization versus time for HDL electrodes, discharged at 30 ma/cm^2 (27.9 amps/ft^2), as a function of temperature. The results were corrected for ir polarization determined at 150 seconds; the broken curve also shows the uncorrected values at -72°F where the ir correction was maximum for this set of results. At room temperature, there is a small polarization (about 20 mv), which is almost constant until the electrode is almost completely discharged; at 0°F there is again a small polarization at first but it increases significantly after the electrode is about two-thirds discharged. As temperature decreases the polarization increases, and the shape of the curve becomes more complex. Figure 4 shows the polarization after 150 seconds of discharge (about 30 percent discharged), which corresponds to the almost flat discharge regions; a marked increase in polarization below 0°F is apparent. Since the correction for the ir effect was also made at this time, the data is reasonably accurately corrected for ir.

The capacity of the HDL electrodes is somewhat variable, which is to be expected for such small electrodes (1/3 cm^2) stamped out from larger sheet samples, since the Ag/Ag_2O cannot be perfectly evenly distributed over the Exmet support. The mean value was 4.89 coulombs (for area of 0.316 cm^2), with extremes of about ± 5 percent. The capacity results were random in variability and showed no trend with temperature or with current density.

Figure 5 shows typical galvanostatic discharge curves (HDL electrodes) at 73°F , and Figure 6 shows curves at -52°F. Values were corrected for ir assuming that the value measured at 1.42 coulombs of discharge applied over the whole curve. This point of discharge corresponds to a region between 1/4 to 1/3 of total coulombs, and corresponds to the minimum polarization in the plateau region following the initial peak polarization. Figure 7 shows Tafel plots of polarization versus log current density at this point. The values for lower current densities were obtained by discharging the electrode at 10 ma/cm^2 until it reached the plateau, then changing the current density to low values and measuring steady polarization at the low currents. A range of current from 0.1 ma/cm^2 to 5 ma/cm^2 was accomplished within the next 1 coulombs of discharge. It was noticed that the initial parts of the curves of Figure 6 were variable from sample to sample, for example, the 30 and 60 ma/cm^2 curves sometimes looked like the 80 ma/cm^2 curve shown, with high initial polarization peak.

Recorder plots such as in Figure 6 do not show fine detail at short times and Figure 8 shows oscilloscope traces for the first few seconds of discharge. Again, the initial peak was more pronounced in some samples than in others. The 58 ma/cm^2 line in Figure 6 contains all of the general features; there is evidence for an initial polarization peak occurring within 10 seconds, followed by a slowly-developing second peak, followed by rapid increase of polarization as the electrode approaches complete discharge. At higher current densities, the two peaks fuze, while at lower current densities the first peak does not develop.

Since the presence of peaks and plateaus varied between samples of HDL electrodes and since the electrodes were prepared by electrolytic charging, it was decided to charge electrodes with anodic current and then perform discharge tests. Figure 9 illustrates typical results of cathodic discharge immediately after anodic charging; the broken line indicates the "normal" values, as found in Figure 8, for example. The regions in the curve can be described by: a is the ir jump; b is rapid rise of polarization due to double-layer charging; c is a plateau of discharge followed by a shallow peak at d; e is a plateau of discharge followed by rapidly increasing polarization as the electrode approaches complete discharge in region f. By prior anodic charging, at potentials much less than the Ag_2O-AgO equilibrium potential, the plateau at c is lengthened proportionately to the coulombs of charge, to c' as shown. In addition, a pronounced peak is developed after b'. The polarization level at e, f is virtually unchanged. If such a charged electrode is left standing at open circuit in the electrolyte, the length of plateau c' decreases with time and comes back to normal values after standing overnight at -54°F. Alternatively, if a normal electrode is discharged to region e just after peak d, allowed to return to open circuit potential, then discharged again at the same current density, the coulombs in region c

is shortened. Then if the electrode is left for some time at open circuit, the length of region c increases again to usual values.

TABLE 1. Characteristics of 50:50 weight percent Ag-Ag_2O Electrodes (T.D. is silver from thermal decomposition of silver oxalate)

Code No.	% Porosity	Silver Type	Thickness, mm	Observed Discharged Capacity, coulombs/cm^2
HDL	70	Electroformed	0.25	15.4
16-TD	16	T.D.	0.312	70.5
65-TD	65	T.D.	0.405	45
63-TD	63	T.D.	0.262	19.5
63-F	63	Fischer	0.51	57
20-F	20	Fischer	0.34	57
81-F	81	Fischer	0.70	27

Table 1 shows the characteristics of a group of electrodes prepared from silver and Ag_2O powder, as described previously. The BET areas of the constituents were 0.57 m^2/g for Fischer silver, 0.45 m^2/g for T.D. silver and 0.60 m^2/g for Fischer Ag_2O. These correspond to equivalent spherical diameters of 1.01μ, 1.3μ and 1.0μ. On galvanostatic discharge at 30 ma/cm^2, -52°F, it was observed that some electrodes gave high initial ir jumps. After some discharge, ir values measured at various points in the discharge were almost constant and usually comparable to previous results, see Table 2. (Although electrode 63-TD gave an effective resistance of 11 ohms which is high compared to the usual values of 4 to 8 ohms, its discharge curve after correction for this value was similar to that of 65-TD.) It must be remembered that these values include the resistance of the electrolyte between test electrode and Luggin capillary (see Figure 2). It can be concluded that high initial ir values decreased to normal values after no more than 2 percent of discharge. It is also concluded that these normal values of ir polarization did not increase even when electrodes were 95 percent discharged.

Figure 10 shows polarization versus degree of discharge, corrected for ir. The marked effect of porosity is apparent; for example, comparing 63-F with 20-F, the 20-F electrode contains more Ag_2O and Ag and is thinner, yet operates at 75 to 200 mv more polarization. There was no correlation between high initial ir values and later performance. Figure 11 shows typical initial time results for the electrodes. A significant polarization peak was observed, similar to that found with the electrolytically charged HDL electrodes, but more pronounced. For some of the electrodes, 81-F for example, part of this peak was due to high initial ir value which decayed during discharge. Even after

allowing for this, a pronounced peak is still present and it is also present in cases, 65-TD for example, where the initial and steady ir values were nearly the same. The shape of the initial polarization curve, when it is not obscured by a high initial ir, contains the a, b, c, d, e, regions discussed previously.

TABLE 2. ir polarization at 30 ma/cm^2 for 0.316 cm^2 electrodes, -52°F.

Electrodes	% discharge	ir polarization mv
81-F	0	240
	45	40
20-F	0	90
	2	62
	20	60
	75	75
	96	75
63-F	0	65
	2	50
63-TD	0	145
	12	110
	80	110
65-TD	0	80
	7	70
	40	67
	70	68
16-TD	0	180
	6	80
	32	80
	60	80
	80	80
	96	80

The effect of the porous nature of the test electrodes was investigated by making thicker electrodes from five of the 10 mil HDL electrodes stacked together. The stack was mounted in the electrode holder in the usual way with one face only exposed. Some preliminary tests, and some theoretical calculations (see Discussion of Results) suggested that 30 ma/cm^2 at -52°F should give a small but significant amount of reaction at the back section and a lot of reaction in the first section. It was also found that there was some evidence for poor electronic contact between the sections, therefore a fine dusting of silver powder was applied between the sections before compressing in the holder. The stack was discharged to about 45 percent of total capacity, disassembled and discharge completed on each of the sections. Knowing the average coulombic capacity of the sections, the amount of the coulombs discharged in each section during the first discharge was readily calculated. The results are shown in Figure 12. Distribution of reaction through the 50 mil thick stack is clearly evident.

Figure 13 shows the polarization of this thick electrode during discharge. If reaction were uniformly distributed through the electrode, a current density of 30 ma/cm^2 would be 6 ma/cm^2 per section. On the other hand, if reaction were concentrated in the outer section, polarization would be similar to that for just one section at 30 ma/cm^2. As expected from Figure 12, polarization lay between these two extremes. Of interest is the more rapid increase in polarization with amount of discharge for the thick electrode.

Figure 14 shows polarization for the remainder of discharge for each section. It can be seen that partial discharge develops the pronounced peak of polarization seen previously at higher current densities. This peak decays on further discharge so that each curve fuzes into a common curve nearer completion of discharge.

DISCUSSION OF RESULTS

Considering first the HDL electrodes produced by electro-forming of sintered silver powder, and considering the internal surface of the electrode before charge to be like an extended solid surface of silver, there are two possible forms in which Ag_2O can be produced. First, the entire surface of the silver can be covered with a tight layer of Ag_2O which grows by solid-state film growth. BET measurements on these electrodes give an area of 0.4 m^2/g of silver, which is approximately 300 cm^2 of internal area per cm^2 of electrode. Thus at 30 ma/cm^2, the true current density would be about 0.1 ma/cm^2. A continuous film of Ag_2O of 0.1μ thick would give a resistance of (10^{-5}) (10^{8}) ohm cm^2 and an ir polarization of (10^{3}) (0.1) = 100 mv. This is an order of magnitude higher than the experimental electronic ir values for these electrodes and it must be concluded that if a continuous film of Ag_2O covers the silver it must be less than 100 Å in thickness. It seems more logical to conclude, from the experiments described by Thirsk (15), that the major part of the Ag_2O formed is in discrete crystalites (which can grow to about 1 μ in size) attached to the Ag surface thus leaving relatively bare silver present to take and supply electrons. It can be argued that whatever is the mechanism of anodic formation or discharge of Ag_2O, it cannot involve charge transfer through thick crystalites or solid layers of Ag_2O, since no large electronic resistance is present.

On the other hand, crystalites of Ag_2O growing over silver surface could form a porous layer with electrolyte in the pores reaching from silver to the exterior of the growth. Ionic conductance would have a resistance, based on the total area, of

$$r = \rho\, q\delta/\theta$$

where ρ is the specific resistance of the electrolyte, q is a tortuosity factor (2), δ is the thickness of the layer, θ is the porosity of the

layer. Assuming that the porous film grows to a set thickness, estimates can be made of ir polarization for various values of θ. For example, taking q as $\sqrt{2}$, ρ as 2 ohm cm, θ as 0.1, δ as 1 micron, the aforementioned 0.1 ma/cm^2 would give only a small fraction of a millivolt of polarization. Thus, ionic ir polarization through such a film would be small at 30 ma/cm^2 discharge unless θ were very low values, 10^{-5} for example. Similarly, the formation current of 2.5 amps/in^2 corresponds to a true current density of about 2.5 ma/cm^2. This would still give negligible ir effects unless porosity were very low.

An alternative hypothesis is that on charge the porous layer of Ag_2O has to transport OH^- ion through contained electrolyte according to

$$2Ag + 2OH^- \rightarrow Ag_2O + H_2O + 2e^-$$

A rough estimate of porosity corresponding to a limiting current condition can be obtained from

$$i_L = \theta DC/q\delta$$

where D is the effective mass transfer factor of hydroxyl ion, cm^2/sec, and C is the concentration in g. moles/cm^3. Assuming D to be approximately 10^{-5} cm^2/sec, C = (7.2) (10^{-3}) g. moles/cm^3, δ = 1μ as before,

$$i_L \approx 50\theta \text{ amps/cm}^2$$

Again, it is concluded that on charge there will be a rapid increase in polarization only when θ becomes very small.

The BET area corresponds to a particle size of the silver making up the electrodes of less than 1μ. The porous electrode would thus behave like a sheet of silver of less than 1μ thick crumpled up into a 10 mil thickness, and if the interior were uniformly used (see below), Ag_2O crystalites growing on the surface would effectively block off the surface only if they overlapped to give very low θ values, since the layer of Ag_2O could not be very much thicker than 1μ. The conclusion is that if transfer of ions through a porous film leads to ir or mass transfer polarization, then this polarization will develop very suddenly as extra charge takes θ from a small value to a very small value. Figure 15 shows anodic charge of the Ag/Ag_2O electrodes at 75°F. At the lower current densities, it is possible to convert almost all of the unreacted silver powder to Ag_2O before the potential rises to AgO formation. At 145 ma/cm^2, however, only about 50 percent is converted before AgO formation potentials.

The plateau of discharge at c in Figure 9 indicates that there is some material which discharges more readily (at lower polarization) than the major amount of Ag_2O present. In the electroformed electrodes this might be ascribed to silver carbonate or silver peroxide, but the typical S shape of b, c, d, is also clearly apparent in the other

electrodes made from reagent grade Ag_2O. One explanation is that thin, continuous layers of Ag_2O cover the silver in the electrode and that these layers are more active than the bulk crystalites of Ag_2O. Assuming that a monolayer has roughly 0.2 m coulombs/cm^2 of capacity, 300 cm^2 of internal surface would give 0.06 coulombs/cm^2 of electrode. Estimates of the amount of charge in region c under normal conditions gives about 0.1 coulombs/cm^2, thus the layers might be only a few molecules thick. After anodic charge at low temperature, region c is increased, possibly representing thickening of the layer. However, on soaking in electrolyte at open circuit the charge in region c returns to about 0.1 coulombs/cm^2, indicating that there is an equilibrium amount of surface film in the $Ag/Ag_2O/KOH$ system of only a few angstroms thick. The solubility of Ag_2O is too small for the plateau to be due to discharge of dissolved oxide in the pores of the electrode. Possibly, this S shape, with a plateau of c, has not been observed in room temperature measurements because operation at low temperatures accentuates the polarization peak at d, thus clearly separating it from the plateau region. It is interesting that similar results at low temperature have been obtained with cathodic discharge of solid silver sheet anodized to Ag_2O formation (16), although the current density to obtain similar voltage-time curves is reduced from 30 ma/cm^2 for HDL electrodes to 0.3 ma/cm^2 for anodized sheet.

Whatever the cause of this initial region of discharge it caused variability in the first time interval of discharge of HDL electrodes which made it difficult to observe quantitative results on the magnitude of peak d as a function of current density and temperature. A general pattern is evident, however; the peak at d is more pronounced at higher current densities and at lower temperatures. If the electrode is partially discharged, allowed to rest at open circuit and then further discharged, the peak is clearly evident, see Figure 14. Alternatively, the peak is clearly present in the pressed powder electrodes, Figure 11. It is not due to the porous nature of the electrodes because it is observed on discharge of anodized silver sheet (16). On the other hand, fairly rapid break-and-make of the current to perform ir measurements show no peak on make, see Figure 8. It can be concluded that the peak reappears only after some stand time.

Three obvious explanations for peak d come to mind. First, by analogy with anodic charging, the peak could be a nucleation polarization. This would fit in with the dependence on current density and temperature. It is not clear, however, what is being nucleated. It could be dissolved silver deposition on preexisting silver by

$$Ag_2O(s) + H_2O \rightarrow [Ag_2O \cdot H_2O] \rightarrow 2Ag^+ + 2OH^- \quad (3)$$

$$Ag(s) + Ag^+ + e^- \rightarrow 2Ag(s) \quad (4)$$

Equation 4 would be the nucleated step. Polarization produces growth of nucleation centers, which are still present after rapid break-and-make

of the circuit. On stand, the growth centers become poisoned by impurity adsorption or decay by molecular rearrangement to a non-nucleating structure.

Second, if the reaction in equation 3 were slow at low temperatures, then the concentration of Ag^+ would decrease with current, giving concentration polarization in reaction 4. The rate of dissolution of Ag_2O could be voltage dependent, increasing with cathodic polarization. The polarization overshoot would then be ascribed to removal of surface impurities which slow down dissolution, or initial removal of stable surface layers leaving more reactive, freshly-formed surface underneath. Third, if reaction 4 had charge transfer polarization, the production of silver during discharge would have an autocatalytic effect. However, the large polarization overshoots would indicate at least a 10-fold increase in silver area as the polarization decreases to the plateau at e, whereas there is 50% of unreacted silver present initially in the electrodes. In addition, silver area produced during discharge does not presumably dissappear on stand, whereas the peak is re-instated after stand at open circuit. This last fact could be explained by postulating that on stand at open circuit the silver becomes covered with a continuous film of Ag_2O. However, we have already argued that plateau c before peak d corresponds to discharge of surface film. We plan to test the autocatalytic hypothesis by making double-layer capacity measurements during periods c, and in the regions d to e to f, since the double-layer capacity will be primarily due to metallic silver.

Further information can be deduced from Figure 4 if it is assumed that electrodes at different temperatures can be compared in the plateau region, with only temperature as the prime variable. Figure 7 indicates that a Tafel-type relation exists and assuming

$$i = I_A \exp(a\mathcal{F}\eta/RT)$$
$$I_A = k \exp(-\Delta H^{\ddagger}/RT) \qquad (5)$$

the apparent activation enthalpy can be obtained from

$$\eta = \frac{\Delta H}{\alpha\mathcal{F}} + \frac{2.3RT}{\alpha\mathcal{F}} \log(i/k) \qquad (6)$$

Applying this relation to the irreversible line in Figure 4, with i constant, gives $\Delta H^{\ddagger} = 14.5$ k cals /g-mole. The apparent exchange current at -52°F from Figure 7 is 0.3 ma/cm^2. From these data, the values of exchange current at various temperatures are shown in Table 3, with values of b (= $2.3RT/\alpha\mathcal{F}$). It must be clearly understood that the data presented here is not sufficient to prove the existence of a change transfer-controlled reaction with the determined kinetic parameter. However, since equation 5 appears to describe the results fairly well, it can be used as a basis for the discussion of distributed reaction in the next section.

TABLE 3. Exchange currents and Tafel slopes as a function of temperature based upon -52°F data.

Temperature °C	°F	°K	Exchange current i_o ma/cm^2	Tafel slope b, volt/decade
21	70	294	540	.117
16	60	289	340	.115
4	40	277	118	.110
-7	20	266	40	.106
-18	0	256	12.7	.101
-29	-20	244	3.3	.097
-40	-40	233	0.74	.092
-51	-60	222	0.16	.087
-62	-80	201	0.03	.083

Equation 3 shows that water is the reactant to be transported from the bulk of the electrolyte through the pores of the porous electrodes to the interior. Even at 31 weight percent of KOH, water is still present in high molar concentration in the electrolyte, and application of the Austin ϕ criteria (10) shows that distributed reaction will be due principally to ohmic effects. This greatly simplifies analysis of the system because an analytical solution exists for this case when η is large enough for the reaction to be considered irreversible. The basic equation (10) for a plane, porous electrode in which the pores are small compared to the thickness of the electrode is

$$d^2\eta/dx^2 = i_o S\rho\{(R/R_b)\ \exp\ (\alpha\eta/b) - (P/P_b)\exp\ [-(1-\alpha)\eta/b]\} \qquad (7)$$

This equation relates the polarization η at a position x (measured from the back face of the electrode) to the distance x, where η is a function of x, $\eta(x)$. S is the electroactive area per unit volume of electrode, cm^2/cm^3; ρ is the effective specific resistance of electrolyte in pores, ohm cm; i_o is the true exchange current density amps/cm^2 at a reactant concentration of R_b and R is the concentration at x, g·moles/cm^3; P_b, P are the corresponding product concentrations. Since water is present in high concentration, $R/R_b \sim 1$, and for the second term of equation 7 negligible,

$$d^2\eta/dx^2 = i_o S\rho\ \exp\ (\alpha\eta/b) \qquad (8)$$

The solution to this equation has been given elsewhere (17) and only the results of significance to the present work will be given. At low values of η (but still large enough for irreversible reaction), the total current density is approximated by

$$i = I_A\ \exp(\alpha\eta/b) \qquad (9)$$

where $I_A = i_o SL$

Thus a normal Tafel region may be seen with an apparent exchange current density, I_A, which represents complete utilization of the interior of the electrode. On the other hand, when reaction is concentrated toward the electrolyte face,

$$i = I_0 \exp(\alpha\eta/2b) \tag{10}$$

where $I_0 = \sqrt{2i_o Sb/\rho\alpha}$

Thus a Tafel slope of double the normal value is predicted, and L does not occur in the apparent current density, as expected if the deep interior of the electrode is not contributing to the current-producing reaction. The simple relations of equations 9 and 10 are quite useful even though they are only approximations. For example, the current at which these two Tafel lines cross can be called the cross-over current, i_c, and

$$i_c = 2b/\alpha L\rho \tag{11}$$

This is an important relation because it does not contain the kinetic parameters of i_o and S and it can be fairly accurately estimated knowing the porosity of the electrode. If the actual current density is much less than i_c, reaction is uniform through the electrode; if it is much greater than i_c, distributed reaction occurs and equation 10 applies.

Figure 16 shows plots of the complete solution to equation 8 compared with the approximate solutions represented by the two Tafel lines. Polarization is plotted in dimensionless form $\eta/2.3b$, where 2.3b is the (log base 10) Tafel coefficient, that is, 0.12 volt at room temperature, $\alpha = 1/2$. The zero of the polarization scale is arbitrarily taken at $i/i_c = 1$; in practice this point would correspond to a definite polarization which would be higher for a lower exchange current, and the zero of the scale is shifted accordingly (17). The maximum deviation in polarization of the complete solution from the two Tafel lines is about 2.3b/4, that is, 30 mv at room temperature.

It must be realized that we do not claim that the current-polarization relation is given exactly by two straight Tafel lines or by the curve in Figure 16, since the equations are derived for an idealized system. However, it seems likely that the equations will apply well enough to aid in deciding what thickness of electrode should be used for a given duty, even if they cannot predict the exact shape of the current-polarization relation.

Table 4 shows values of I(0)/I(L), I(1/2)/I(L) versus i/i_c, where I(0)/I(L) is the ratio of the specific currents at x = 0 and x = L, I(1/2)/I(L) the ratio of specific currents at x = L/2 and x = L. These represent the relative rates of reaction at these positions, obtained from the solution of equation 8 with the appropriate boundary conditions (17). As expected, as i/i_c increases, reaction is less and less uniform throughout the electrode.

TABLE 4: Calculated values of $I(0)/I(L)$, $I(1/2)/I(L)$ versus i/i_c

i/ic	I(0)/I(L)	I(1/2)/I(L)
0.010	.990	.995
0.169	.852	.888
0.273	.772	.817
0.410	.682	.746
0.588	.594	.671
1.005	.427	.517
1.83	.249	.333
3.09	.132	.193
4.62	.072	.113
10.10	.020	.035

Considering the conditions for the data in Figure 12, the specific conductivity of electrolyte is 20 ohm cm, and L is 50 mil = 0.127 cm. The labyrinth factor (q/θ) can be taken as about 2 giving ρ = 40 ohm cm. From the Tafel slope of 85 mv, $b/\alpha = 0.085/2.3 = .037$ volts. Thus $i_c = 14.6$ ma/cm^2, and Table 4 predicts that a current density of 30 ma/cm^2 would give $I(0) : I(1/2) : I(L) :: 0.22 : 0.3 : 1$. Figure 12 gives the relative rates of reaction as roughly 0.25 : 0.4 : 1. This is a remarkable agreement bearing in mind that the reactive surface is undergoing change during the discharge, and that the transfer factor may also be changing during discharge. A more exact way of comparing theoretical with experimental results is as follows. The solution to the equation enables the fraction of the reaction occurring between 0 and x to be calculated, or the fraction between x_1 and x_2, for any value of i/i_c.

In a later and more complete report, we will give extensive tabulated solutions which will enable the appropriate data to be readily picked out. The specific solution to be used here is that the fraction of reaction, $i(x)/i$, occurring between 0 and x is related to the total current density (i), the cross-over current (i_c), and fractional position in the electrode (x/L), by

$$i/i_c = X \tan X \tag{12}$$

$$i(x)/i = \tan\left(\frac{x}{L} X\right)/\tan X \tag{13}$$

X is an intermediate in the calculation, defined by equation 12. Values of $i(x)/i$ can be compared directly with the experimentally determined fraction of reaction occurring in the various slices making up the electrode. Table 5 gives results for electrodes made of two sections.

TABLE 5. Predicted versus experimental values of percentage of reaction in each electrode section.

Temp. °F	i ma/cm^2	Electrode Thickness cm	i/i_c	Percentage of Reaction in Electrode Section: Back Section predicted	Back Section exptl.	Front Section predicted	Front Section exptl.
-35	150	.050	2.25	29	24.	71	76
-35	100	.050	1.50	35	36	65	64
-35	30	.050	.45	42	40	58	60
-35	0	.050	.15	49	49	51	51
-52	50	.050	1.35	35	43	65	57

It can be seen that agreement between predicted and experimental is good. The percentage of reaction occurring in each section of the 50 mil stack of Figure 12 were predicted to be 11.6, 13, 16, 22, 38; the experimental values were 11, 13, 17, 25, 34.

The above results gives us some confidence in predicting the effect of distributed reaction for one electrode thickness. At -52°F, the estimated value of i_c for the 10 mil thick HDL electrode is 73 ma/cm^2. For 30 ma/cm^2, i/i_c is 0.41 which corresponds to I(0)/I(L) of about 0.7; the predicted increase of polarization above a uniform reaction condition is about 11 mv. Thus at 30 ma/cm^2, a distributed reaction effect is present but it is not very great. At higher temperatures or at lower current densities, the distributed reaction effect is negligible for the HDL electrodes. Similar reasoning can be applied to the electrolytic forming of the 10 mil electrodes, which was carried out at 200 ma/cm^2 on each side of the electrode; this corresponds to an electrode used with current on one face with thickness 5 mils. At room temperature, the effective specific resistance of electrolyte can be estimated at about 10 ohm cm, giving an estimate of i_c of about 500 ma/cm^2. Again the value of i/i_c of 0.4 corresponds to a greater rate of production of Ag_2O at the electrolyte face than in the interior and the ratio of Ag_2O to Ag in the outer face will be somewhat higher than the average of 50 : 50, while it will be somewhat less in the interior.

The above calculations also go some way in explaining the effect of porosity shown in Figure 10. The more porous electrodes will avoid distributed reaction at these conditions, whereas the 20 percent porous electrodes will be undoubtedly in the completely distributed reaction condition and will have higher polarization at a given state of discharge because only part of the electrode interior is being utilized. When the reaction is concentrated at the outer face, a layer of fully discharged material will build up over the electrolyte face and this layer will grow thicker into the electrode as discharge proceeds. Figure 13 indicates that at the point where discharge of th

50 mil stack was stopped, polarization was increasing quite rapidly. Figure 12 shows that this corresponded to complete discharge of the outer face of the electrode. It is possible that this fully discharged layer is relatively impermeable, giving an additional ir polarization for ionic transport. Because of the double layer capacity of this porous layer, this type of ir polarization will not disappear instantaneously when current is interrupted. (This postulate will be tested in future work by fully discharging a 10 mil electrode, making it the outer face of a 50 mil stack, and discharging the stack.)

Again, the concept of distributed reaction goes part of the way to explaining region f in the discharge. The evidence is that polarization increases more rapidly with the state of discharge when the reaction is concentrated toward the outer face. At lower currents and higher temperatures, a more extended plateau of region e is seen, followed by sudden development of region f at high percentage discharge. As current is increased or temperature decreased, region f starts at a lower percent of discharge and is more spread out.

There are probably several reasons for the increase of polarization in region f. Certainly, much increased polarization is expected when the state of discharge has progressed to the point where the active area of Ag_2O present in the electrode is too small to support current. However, the Tafel relation indicated in region e suggests that a simple charge-transfer reaction is rate-controlling. It has already been argued that this cannot involve a reaction occurring on an Ag_2O crystal, since the Ag_2O is non-conductive, would not have a simple double-layer on its surface, and would not give simple Tafel-type rate relations. Thus it appears that the reaction of equation 4 is the likely candidate.

$$Ag(s) + Ag^+ + e^- \rightarrow 2\ Ag(s) \qquad (4)$$

(This will be examined further by varying the area of silver by orders of magnitude keeping other parameters constant, and determing the effect on polarization.) The influence of Ag_2O would occur only via its production of dissolved Ag^+. If the rate of dissolution of Ag_2O from the crystalites (electro-formed electrodes) or powder (pressed electrodes) of Ag_2O is large, the concentration of Ag^+ in electrolyte in the pores of the electrode would be maintained constant until almost all of the Ag_2O had been reacted.

If the above postulate is correct, increased activation polarization can be obtained (at low temperatures where the polarization corresponds to irreversible reaction) by decrease in the concentration of Ag^+. This could arise from a slow rate of dissolution, or from a slow rate of mass transfer to the conductive silver matrix. Examining this last hypothesis, it is difficult to give a mean diffusion path from the surface of an Ag_2O particle to the surface of an adjacent Ag particle (18). In electro-formed material, the crystals of Ag_2O are presumably in contact with Ag, and the mean distance must be of the order of 1 micron.

or less. In the powder electrodes, if the elementary particles of Ag_2O and Ag are well mixed, the distance will again be of the order of 1 micron. However, if an agglomerate of Ag_2O particles touches an agglomerate of Ag particles, the mean diffusion path might correspond to the agglomerate size rather than the particle size.

Using the solubility-diffusivity results of Miller (19), the room temperature values are about (3) (10^{-4}) moles Ag_2O/liter and (3) (10^{-6}) cm^2/sec. Taking a value of 100 cm^2 as a conservative estimate of the internal area of 1 cm^2 plane of the electrode, the steady-state limiting current due to mass transfer of Ag_2O across a diffusion path of 1μ is

$$i_L \approx (10^2)\ (2)\ (96500)\ (3)\ (10^{-7})\ (3)\ (10^{-6})/(10^{-4})\ amps/cm^2$$

$$- 180\ ma/cm^2\ plane$$

As temperature decreases, the diffusion coefficient will decrease comparably to the increase in electrolyte resistivity and the solubility may also decrease. Thus the order-of-magnitude calculation shows that region f at the higher current densities and lower temperatures might involve mass transfer limitations of dissolved silver between an Ag_2O surface and an adjacent silver surface within the electrode. This mass transfer effect would not be altered by stirring the electrolyte except inasmuch as stirring could move electrolyte within the micropores of the electrode. Presumably this mass transfer effect becomes more important as the electrode discharges because, the smaller particles of Ag_2O are consumed first leading to an increased mean diffusion path.

CONCLUSIONS

At low temperatures the galvanostatice discharge curve in general contains five regions of polarization with time; a, b, c, d, e, f. Region a represents an immediate ir polarization, due primarily to the electrolyte path between the test and Luggin tip. Region b is double-layer charging, and is followed by a short plateau c which corresponds to discharge of some active material. Region c progresses into a polarization peak at d, which is not due to ir effects, and is probably a nucleation overpotential. After the peak, a plateau at region e is obtained which appears to correspond to an activated, charge-transfer reaction, possibly $Ag(s) + Ag^+(aq) + e^- \rightarrow 2\ Ag(s)$. In this region the active area of silver is not changing very much.

Finally, the polarization again increases as the electrode tends to more complete discharge, region f, which again is not due to an increased electronic ir effect. If the electrode current density and temperature are such as to cause distributed reaction, the electrode reacts more toward the face, giving increased polarization and a more rapid onset of region f. The increased polarization in region f may be due to layers of discharged material formed at the electrode face

and to mass transfer of dissolved Ag_2O from Ag_2O surface to Ag surface.

Although the work in this report is obviously not a comprehensive picture of how this electrode behaves at low temperature, the plateau region for steady discharge can be fairly quantitatively considered. First, the current density-polarization relation is the Tafel relation

$$\eta = b \log i - b \log I_A \tag{14}$$

where I_A is given by

$$I_A = i_o SL$$

and the temperature coefficient of i_o is $\exp(-14.5/RT)$. In order to get lower polarization (loss of ideal potential) at a fixed temperature, the apparent exchange current I_A must be increased. This can be done by increasing the thickness L (but see below), or by increasing the specific reactive area S by using very fine Ag and Ag_2O powder. The thickness L should be less than a value L_c defined by

$$\begin{aligned} i_m &< i_c \\ &< 2b/\alpha L_c \rho \end{aligned} \tag{15}$$

where $\alpha = 1/2$ for our results, and i_m is the maximum current density of operation. Thicker electrodes will give lower polarization when $i << i_m$, but the value of i_c is reduced when $i_m \geq i_c$, the reaction is concentrated toward the outer face, and polarization increases rapidly with increased i.

It is essential to design electrode thickness and porosity to avoid entering into region f at the outer face when the electrode is only slightly discharged in the interior, for then the polarization increases rapidly with time during discharge. The effect of porosity is contained within the factor ρ, which is the effective specific resistance of electrolyte within the electrode. This factor appears to increase rapidly as porosity is decreased, thus causing a smaller i_c. To avoid this effect, porosities of 60 to 80% should be used. These high porosities reduce the value of S and the coulombic capacity of the electrodes so, again, a balance must be made between the various factors dependent on the conditions of operation and the duty required.

REFERENCES

1. Austin, L. G., Trans. Faraday Soc. (London), 60, 1319 (1964).

2. Austin, L. G., Handbook of Fuel Cell Technology, ed. C. Berger, Prentice Hall, Inc., New Jersey, p. 1 (1968).

3. deLevie, R., Advances in Electrochemistry and Electrochemical Engineering, ed. P. Delahay and C. W. Tobias; 6, 359, (1967).

4. Austin, L. G. and Gagnon, E. G., Report No. 2, October, 1966, Contract No. DA 49-186-AMC-197(D), United States Army Materiel Command, Harry Diamond Laboratories, Washington, D. C.

5. Fleischman, M. and Thirsk, H. R., Advances in Electrochemistry and Electrochemical Engineering, Vol. 3, ed. P. Delahay, Interscience Publishers, Inc., New York, p. 123 (1963).

6. Vermilyea, D. A., Advances in Electrochemistry and Electrochemical Engineering, Vol. 3, ed. P. Delahay, Interscience Publishers, Inc., New York, p. 211 (1963).

7. Dirkse, T. P., and Werkema J. Electrochem. Soc. 106, 88 (1959).

8. Cahan, B. D., Ockerman, J. B., Amlie, R. F. and Ruetschi, P., J. Electrochem. Soc., 107, 725 (1960).

9. Dirkse, T. P., J. Electrochem. Soc., 107, 859 (1960).

10. Wales, C. P. and Burbank, D., J. Electrochem. Soc., 112, 13 (1965).

11. Hamer, W. J. and Craig, D. N., J. Electrochem. Soc., 104, 206 (1957).

12. Austin, L. G. and Almaula, S. C., Report No. 10 Contract No. DA 49-186-AMC-146 (D), United States Army Materiel Command, Harry Diamond Laboratories, Washington, D. C., May (1966).

13. Morrell, D. H. and Smith, D. W., Proceedings of The 5th International Symposium on Power Sources, Pergamon Press, New York (1967).

14. Schroeder, J. E., Pouli, D. and Seim, H. J., 154th Meeting A.C.S., Division of Fuel Chem. Preprints, Sept. 10-15, Vol. 11, No. 3, p. 81-90, (1967).

15. Thirsk, H. R. and Lax, D., paper presented at The Montreal Meeting of The Electrochem. Soc., October 6-11, (1968).

16. Pauli, W., Harry Diamond Laboratory, Washington, D. C., private communication.

17. Austin, L. G., paper in preparation.

18. Austin, L. G., I. and E. C. Fundamentals 3, 321 (1965).

19. Miller, B., paper presented at The Montreal Meeting of The Electrochem. Soc., October 6-11 (1968).

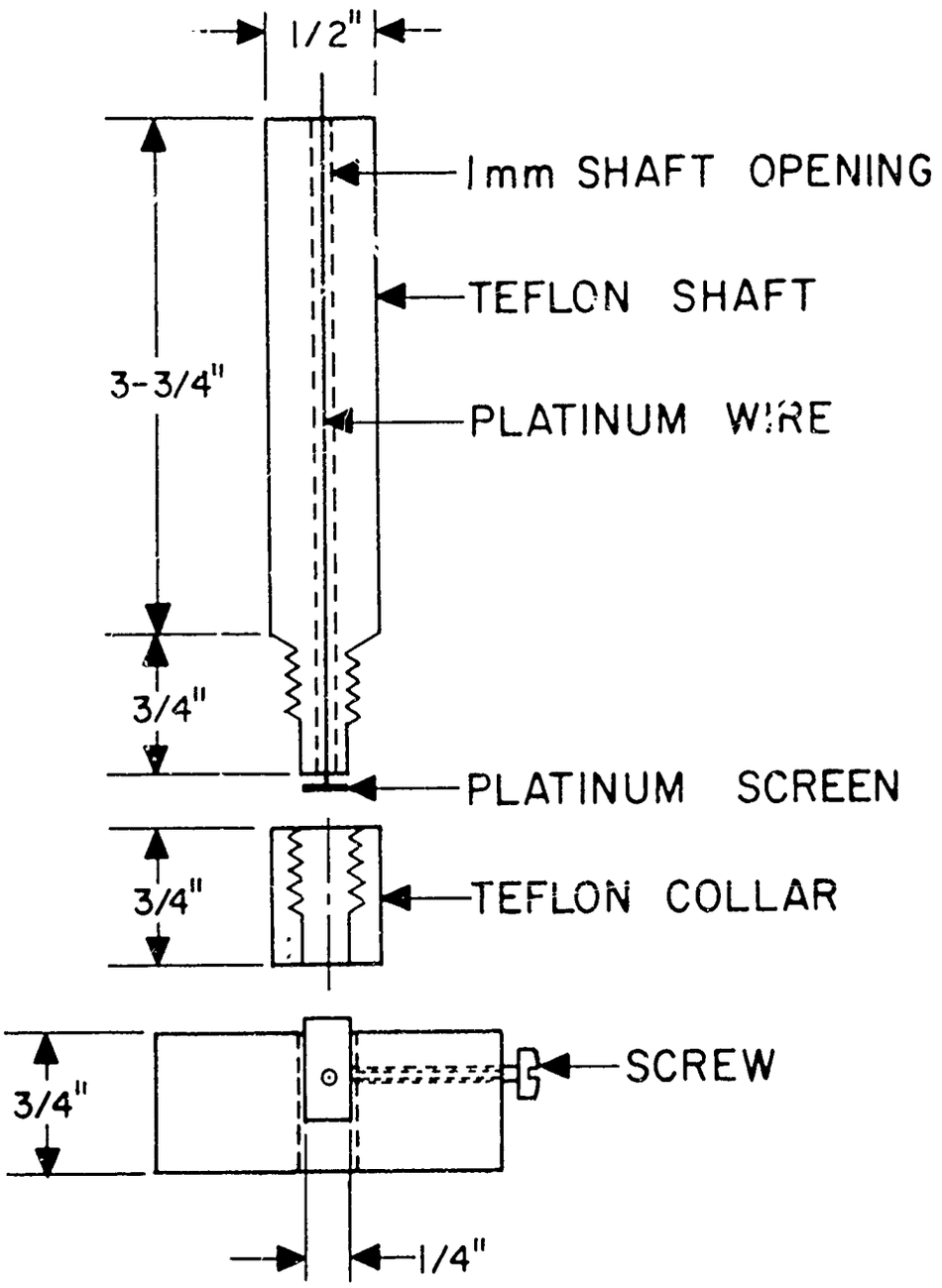

Fig. 1 Electrode holder

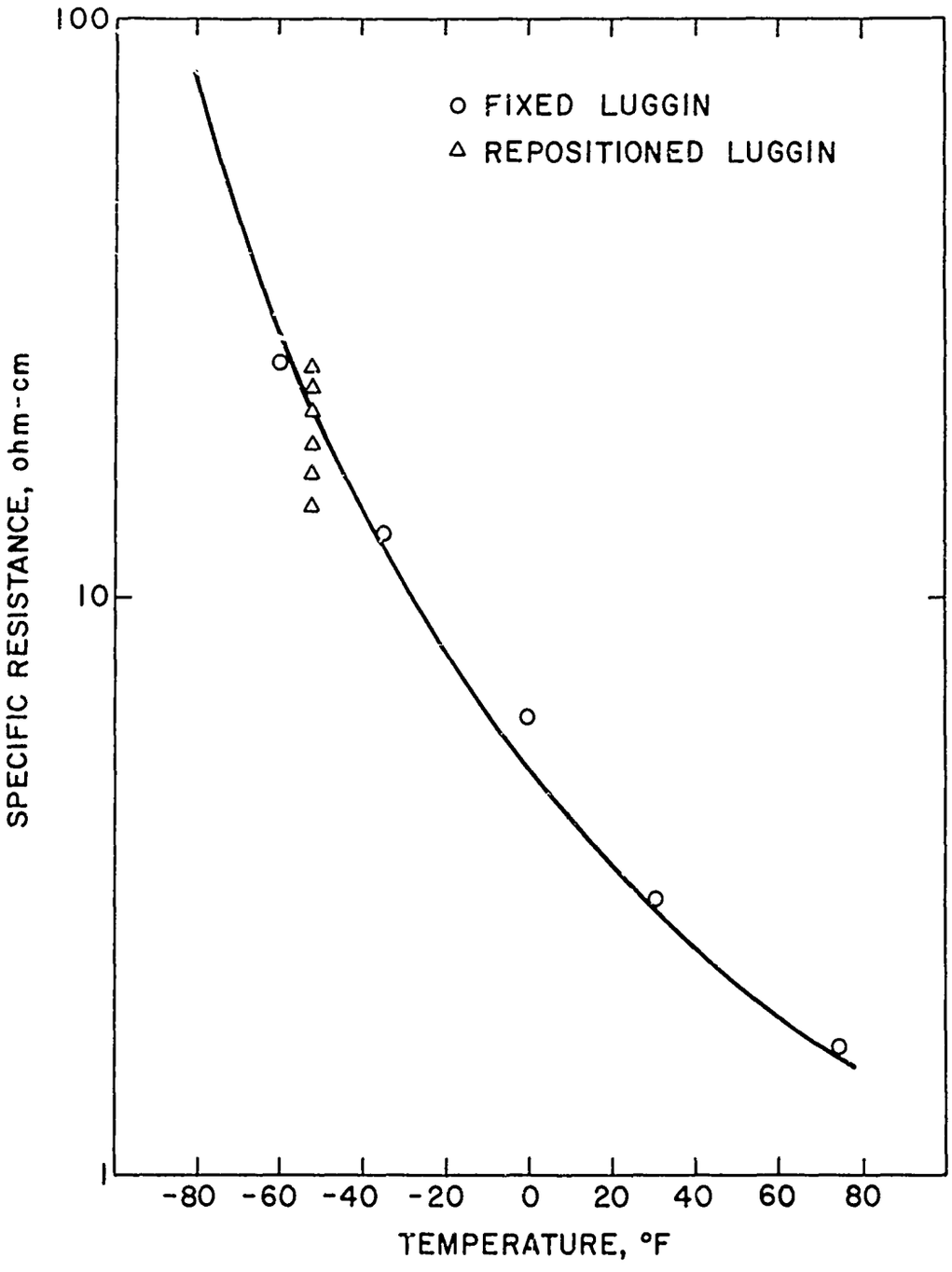

Fig. 2 Specific resistance of 31 weight percent KOH (solid line) and effective resistance (times three) between test electrode and the Luggin capillary.

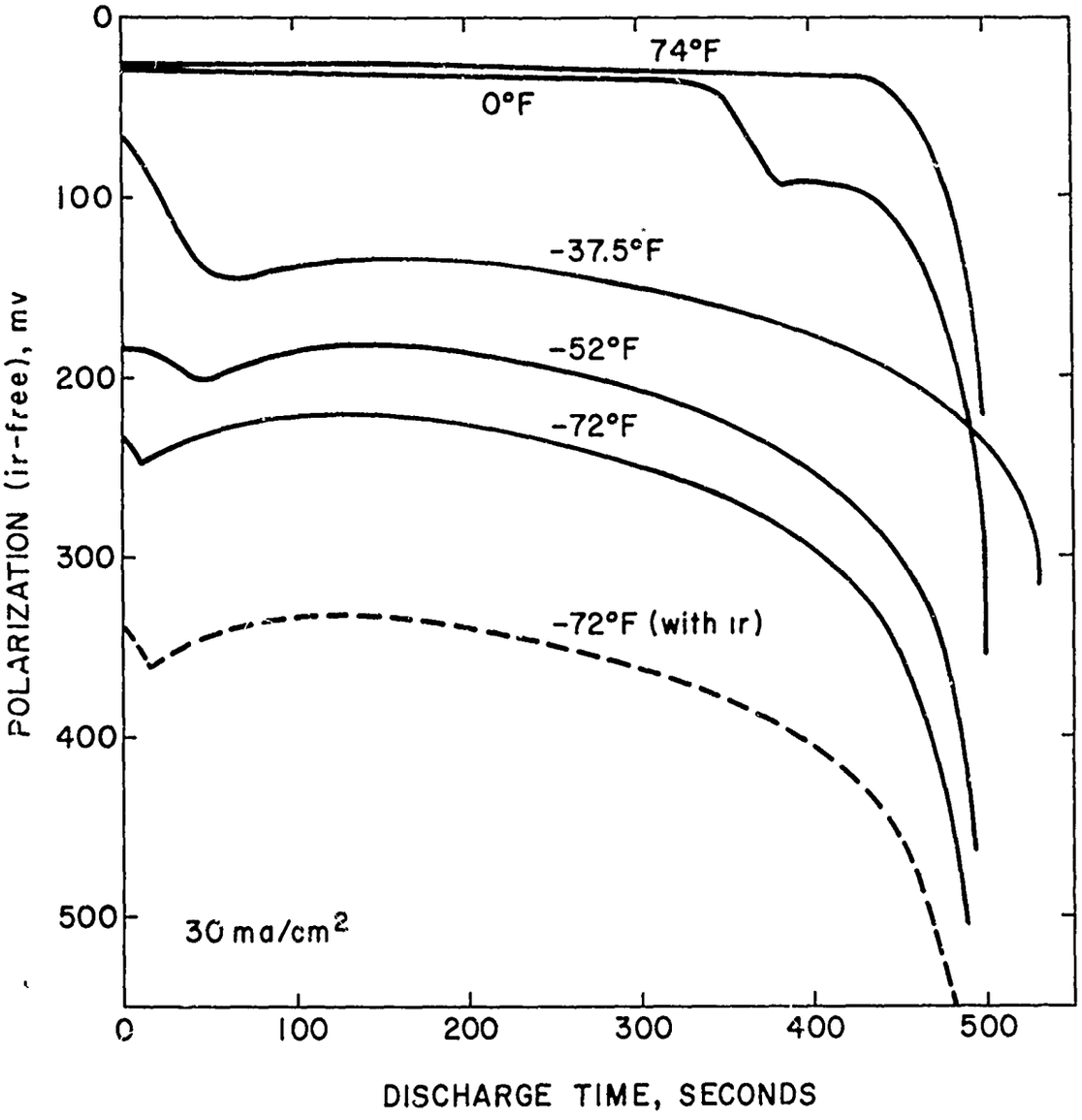

Fig. 3 Galvanostatic discharge at 30 ma/cm^2: H.D.L. electrodes.

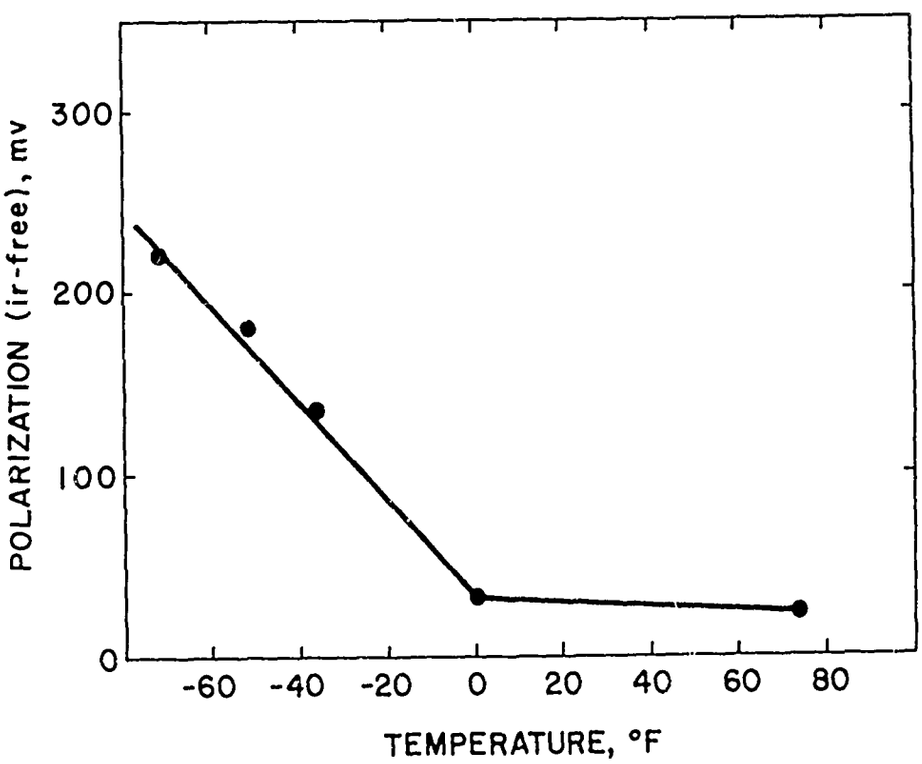

Fig. 4 Polarization (ir-free) at 30 ma/cm^2, measured at about 4.5 coulombs/cm^2 of discharge.

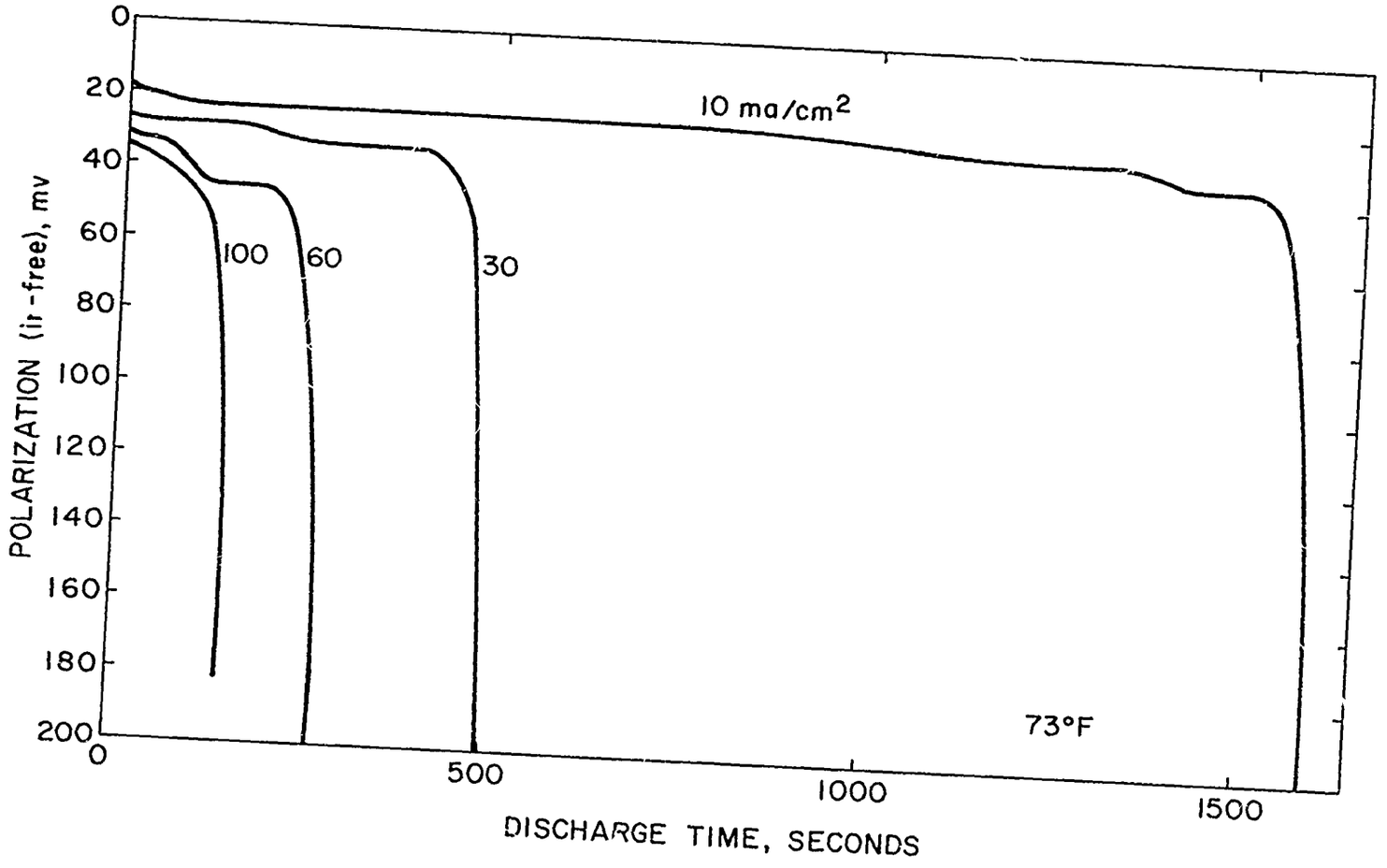

Fig. 5 Galvanostatic discharge at various current densities: H.D.L. electrodes at room temperature.

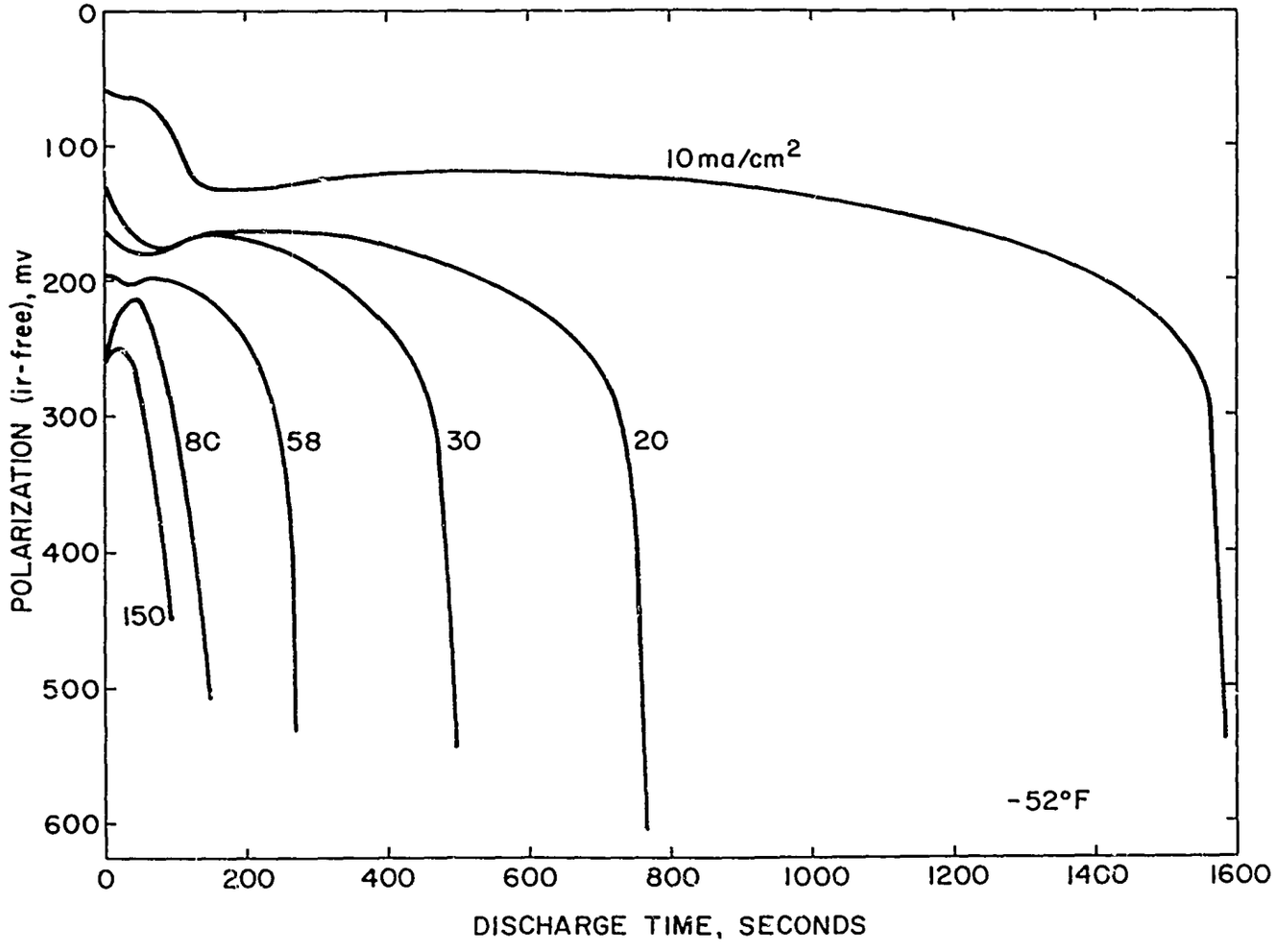

Fig. 6 Galvanostatic discharge at various current densities: H.D.L. electrodes at -52°F.

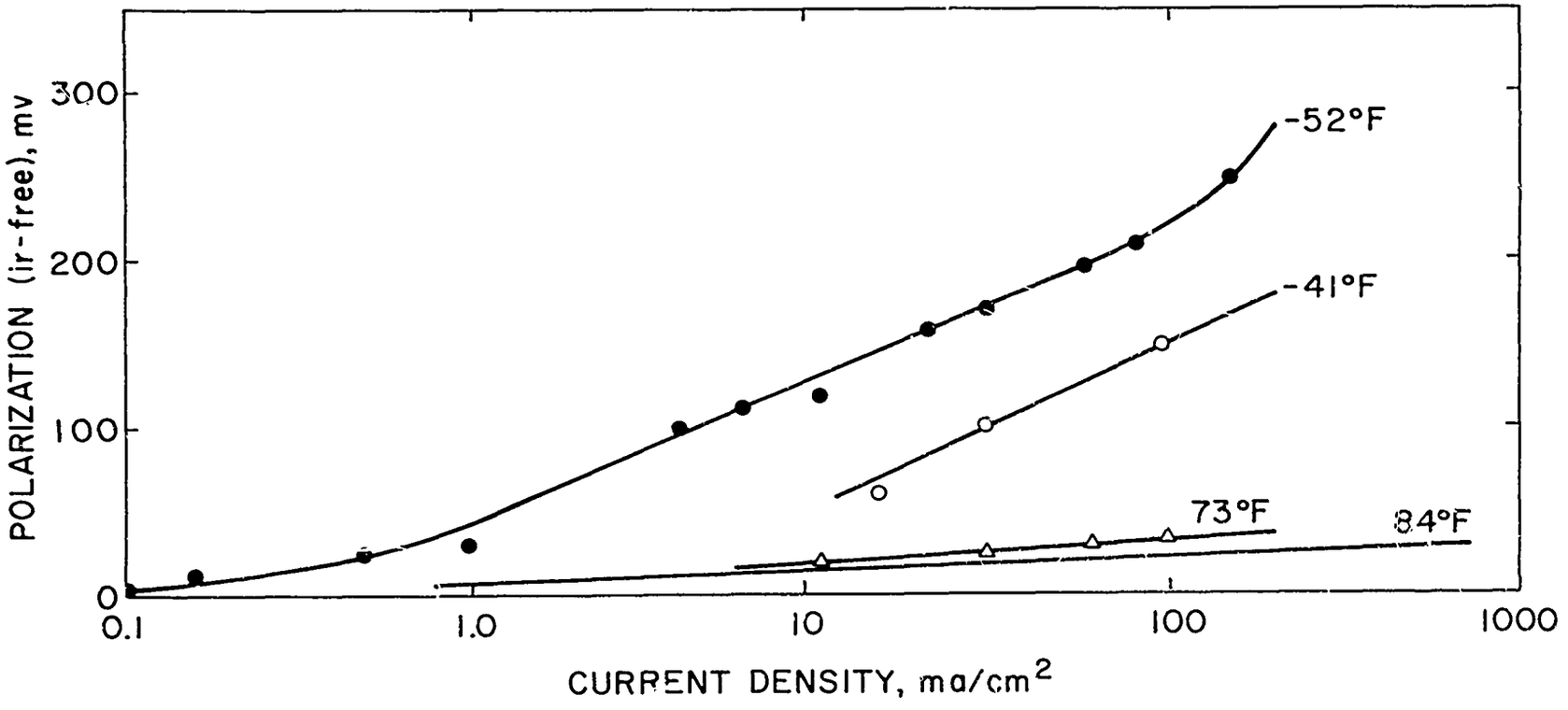

Fig. 7 Polarization versus log current density: H.D.L. electrodes.

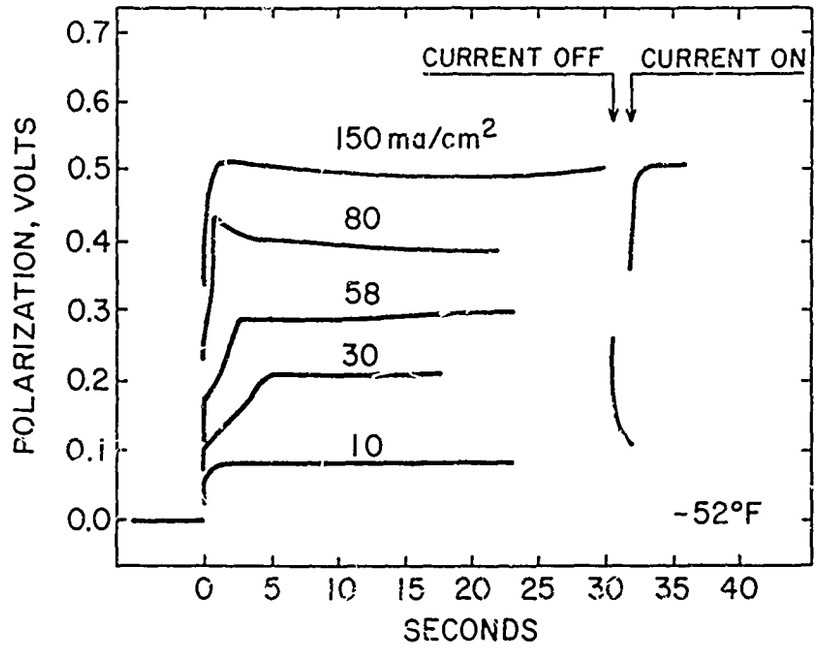

Fig. 8 Oscilloscopic traces showing the initial discharge characteristics of the curves shown on Fig. 6.

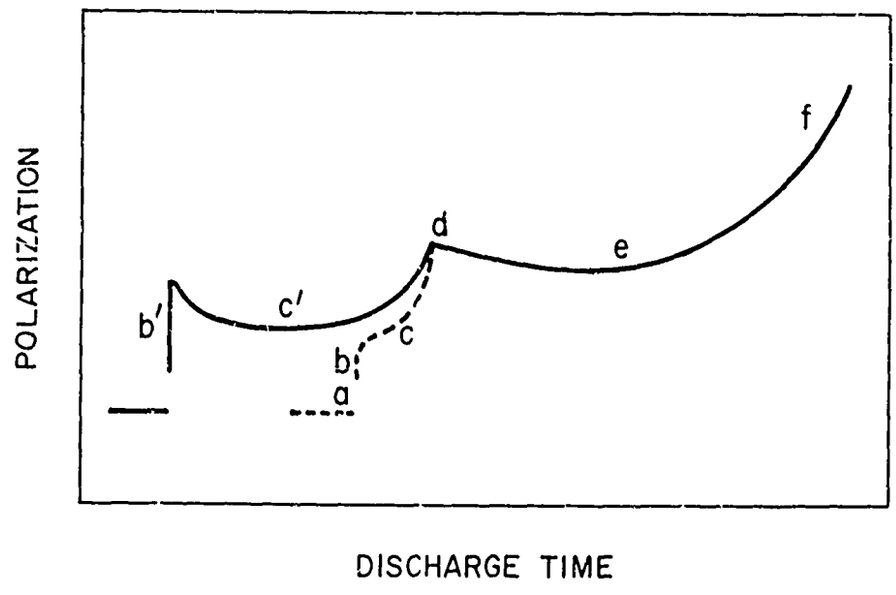

Fig. 9 Illustration of results obtained after electroformed electrodes were anodically charged prior to discharge.

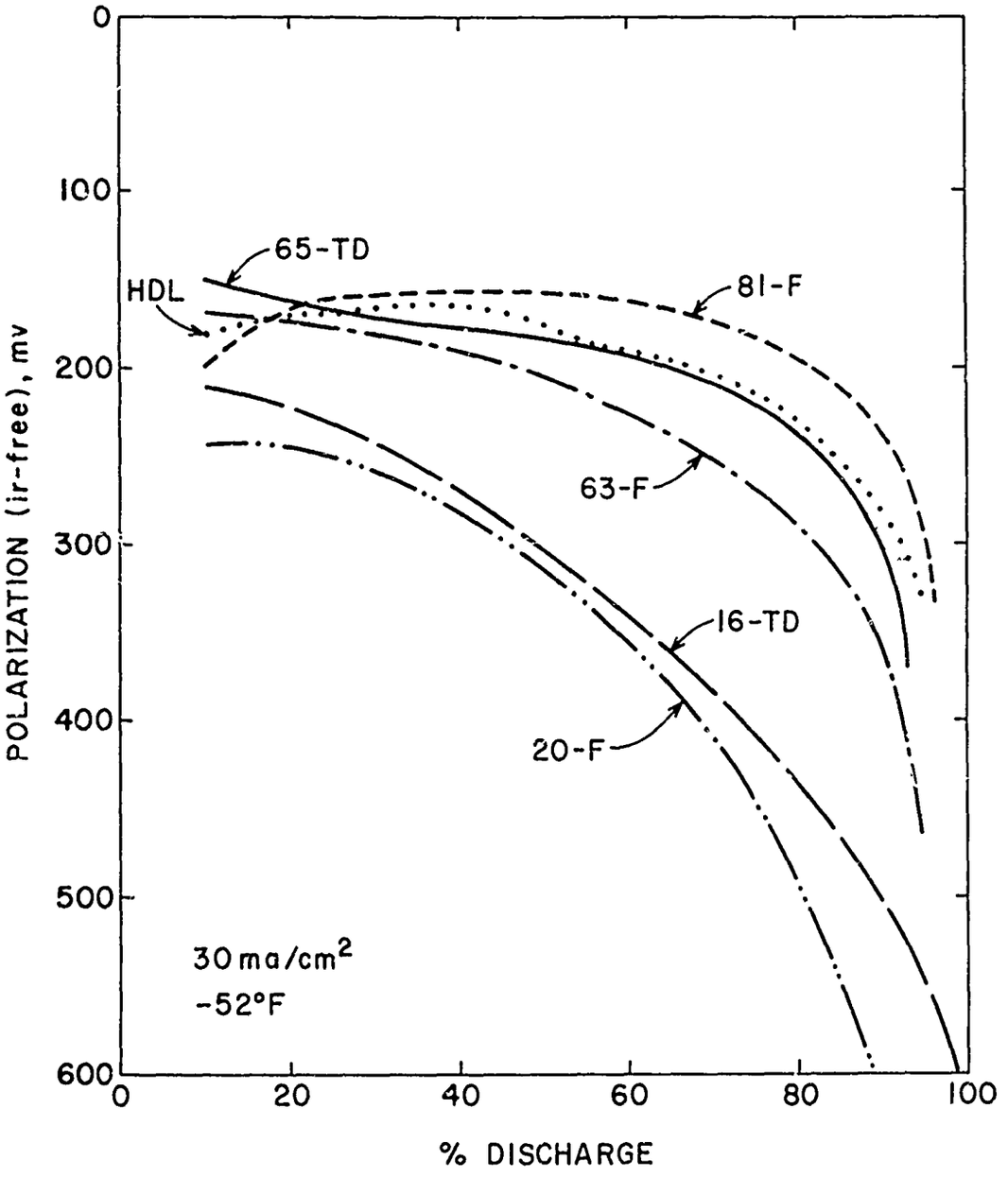

Fig. 10 Polarization versus degree of discharge for pressed $Ag-Ag_2O$ powder electrodes.

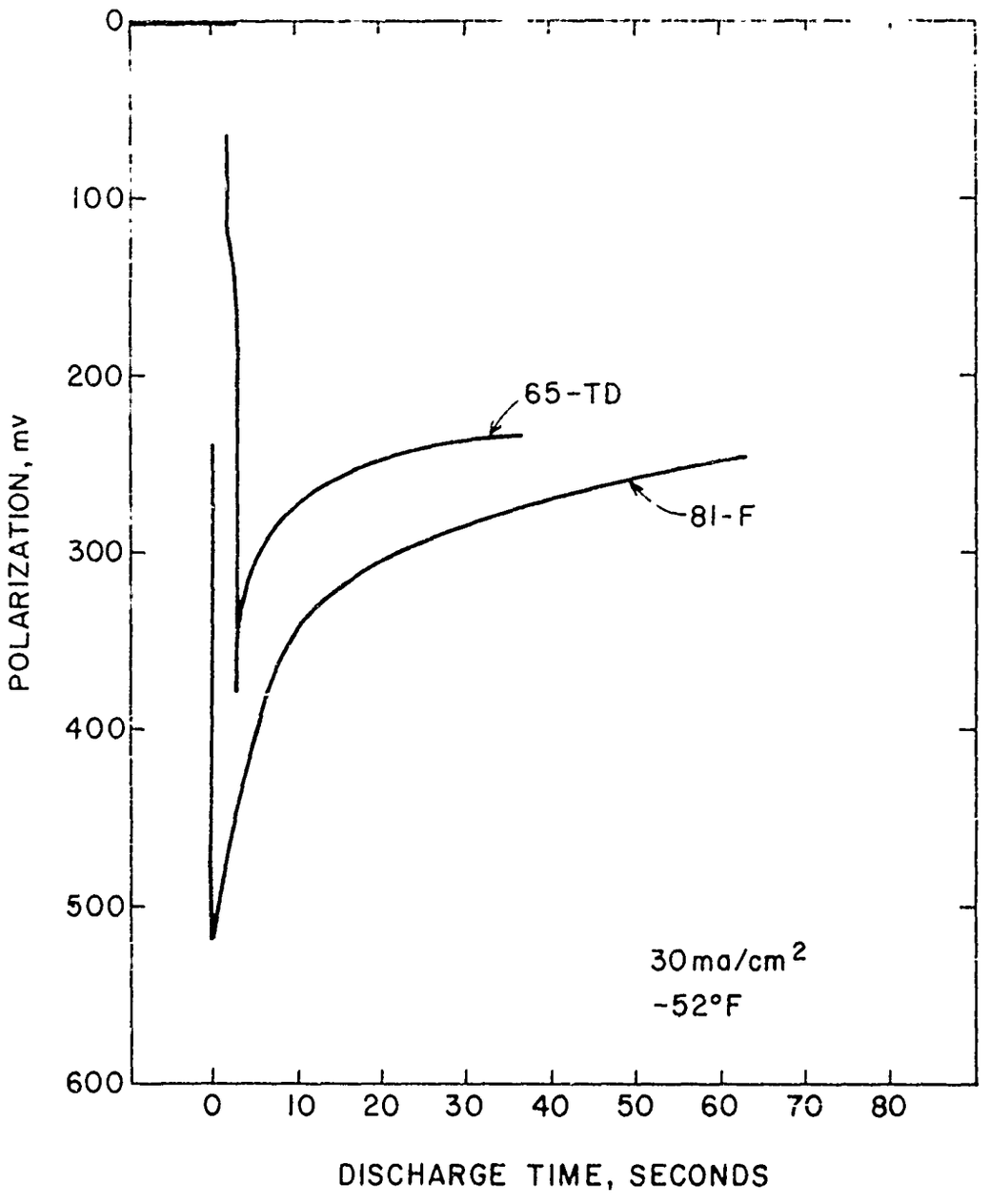

Fig. 11 Oscilloscopic traces showing initial discharge characteristics of electrodes 65-TD and 81-F.

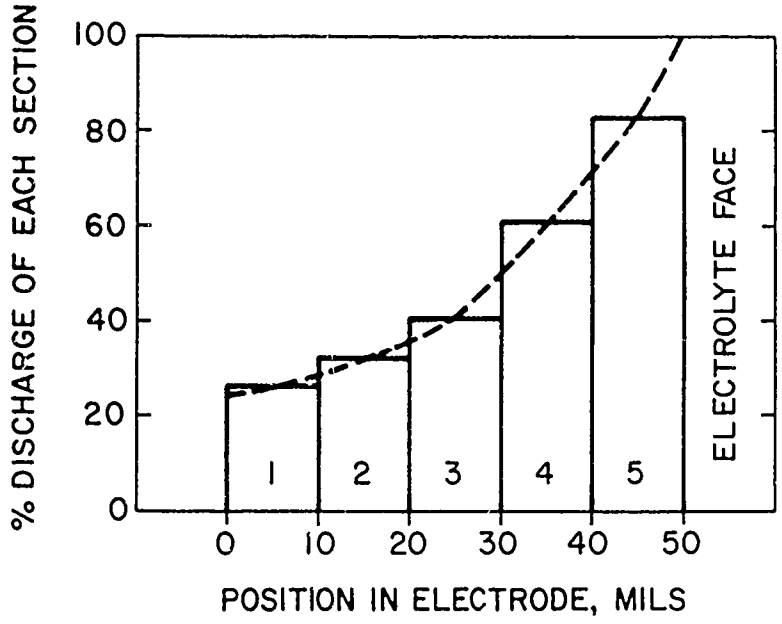

Fig. 12 Distribution of reaction at -52°F through a 50 mil thick electrode.

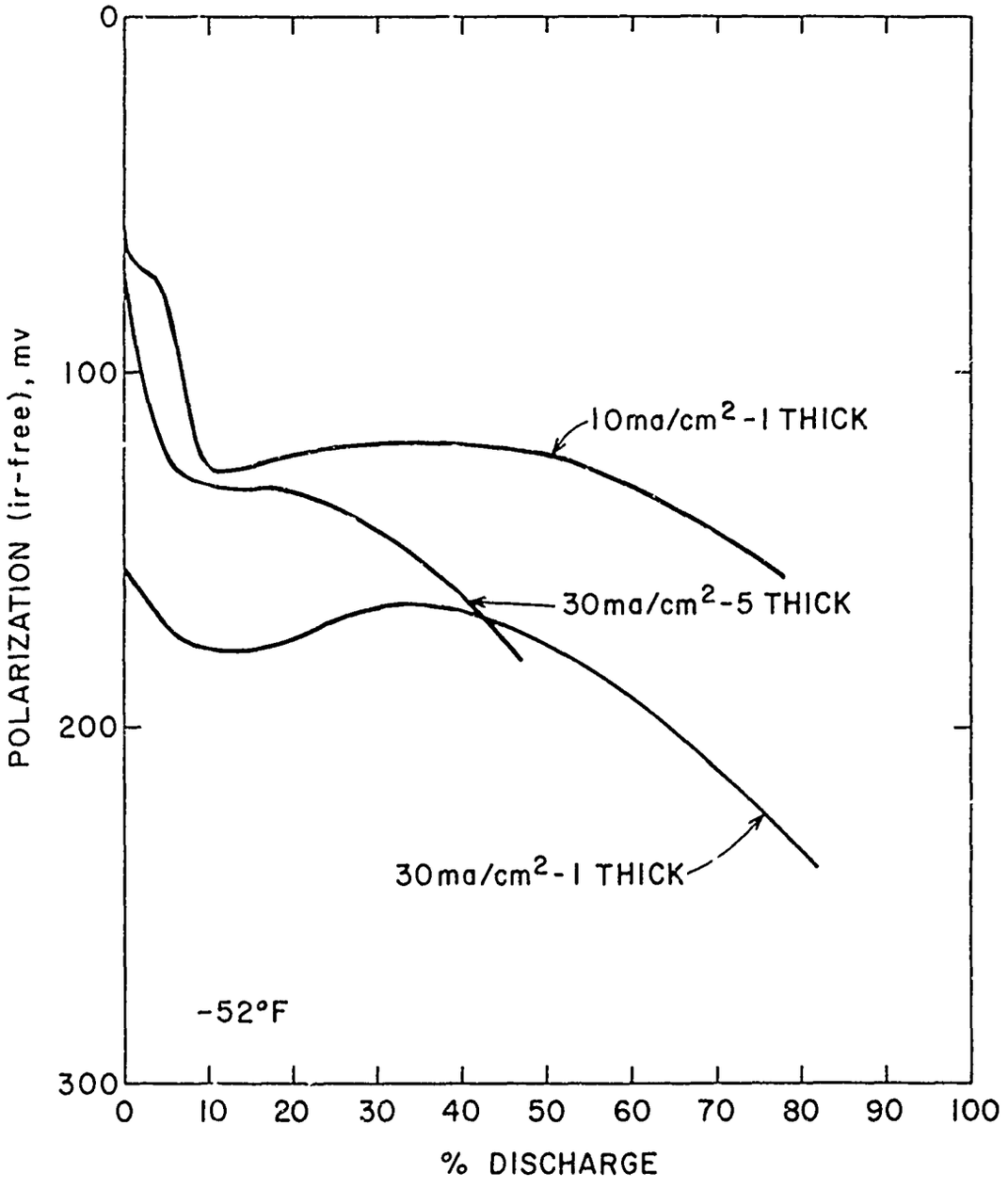

Fig. 13 Galvanostatic discharge for various thicknesses of H.D.L. electrodes; 30 ma/cm^2 and -52°F.

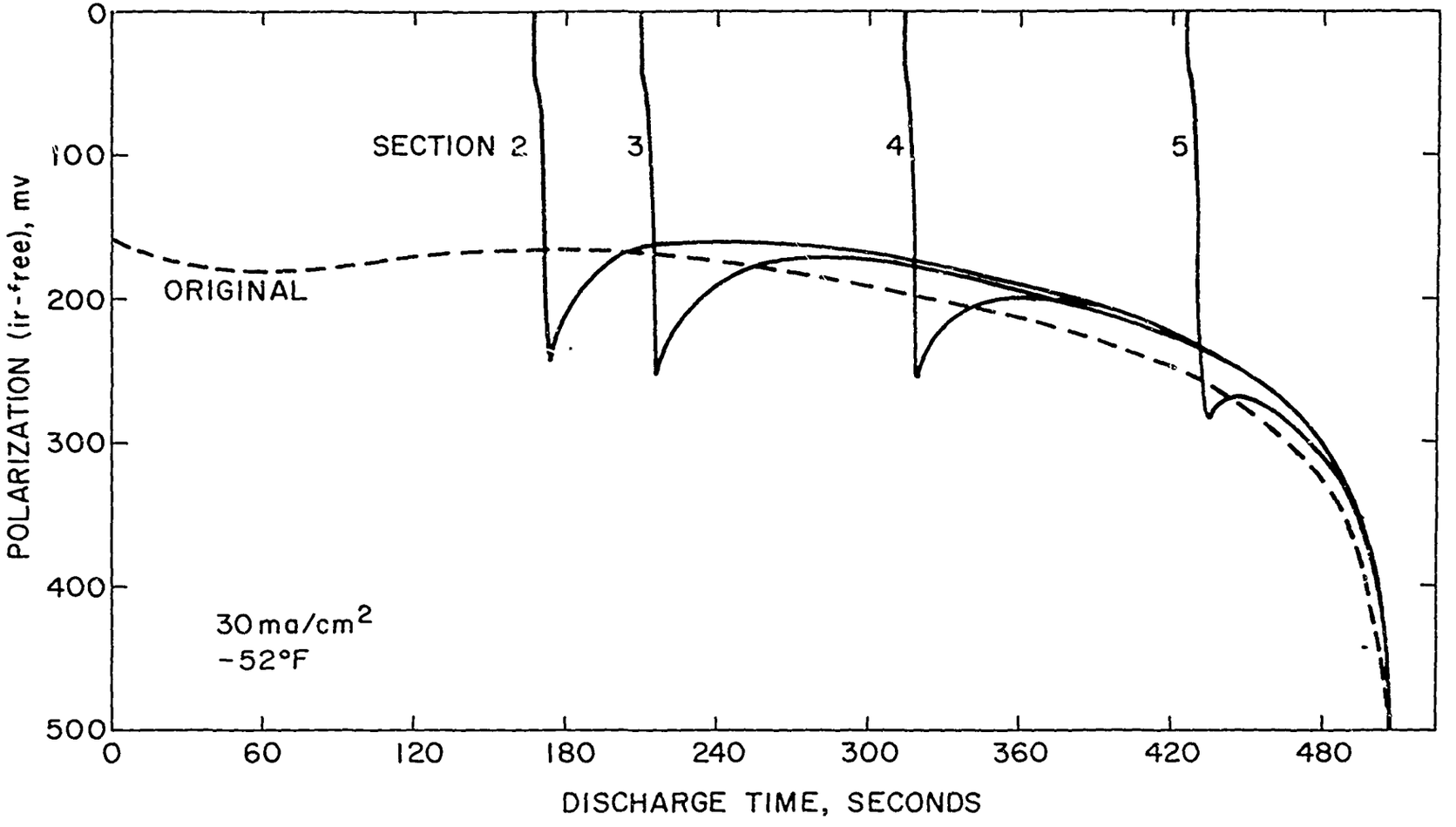

Fig. 14 Galvanostatic discharge of individual electrodes used in the stacked electrode experiment.

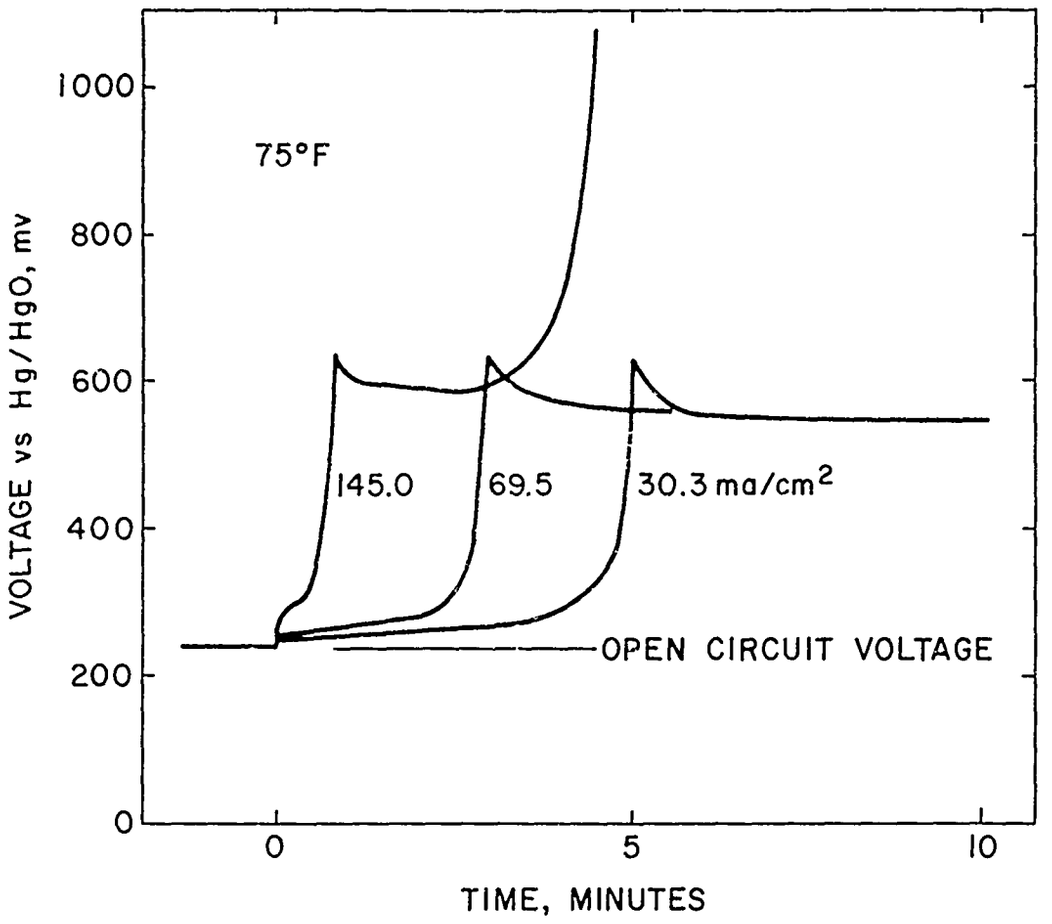

Fig. 15 Anodic charge of H.D.L. electrodes at room temperature.

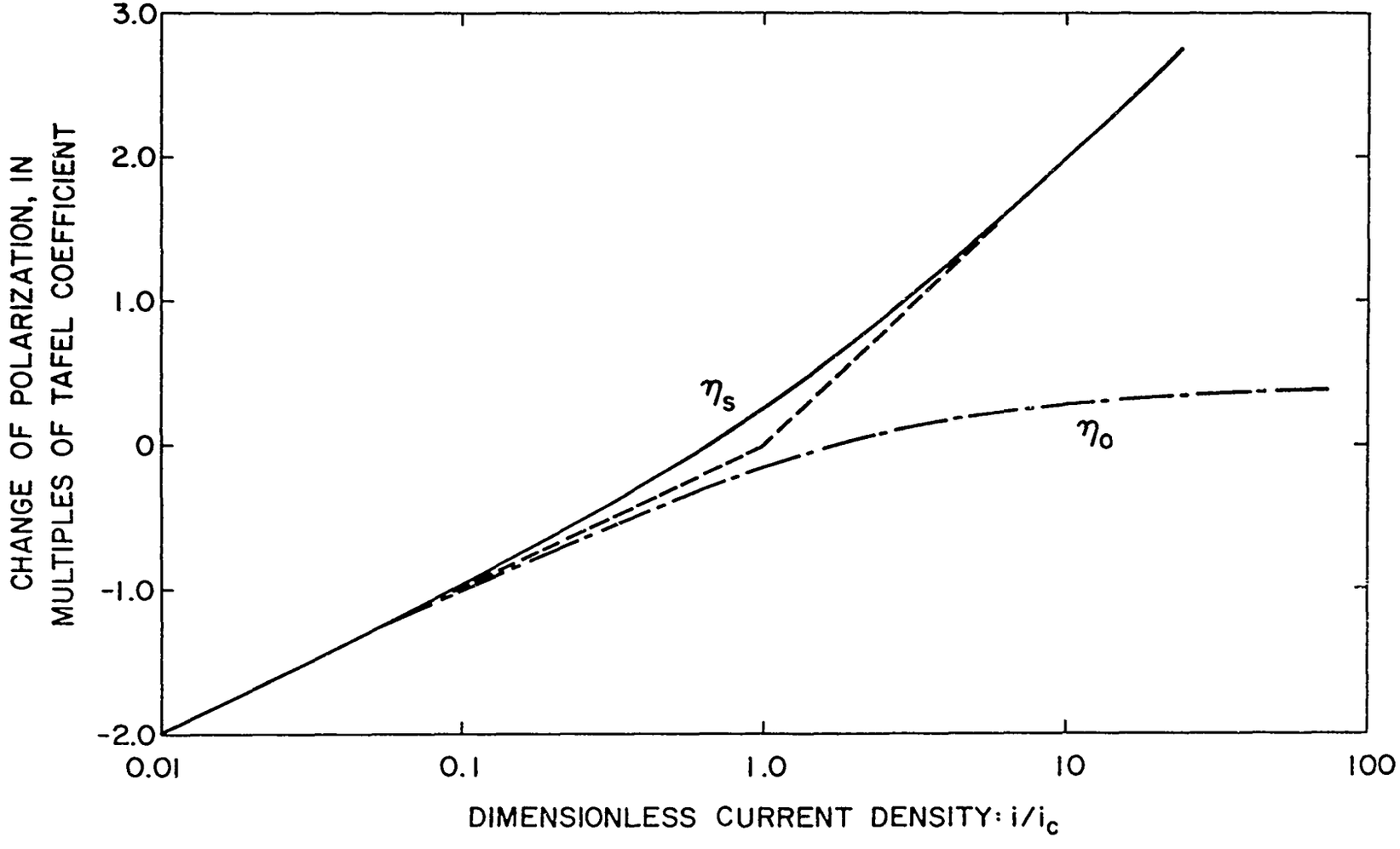

Fig. 16 Dimensionless plot of solution to equation 8.

UNCLASSIFIED
Security Classification

DOCUMENT CONTROL DATA - R & D

(Security classification of title, body of abstract and indexing annotation must be entered when the overall report is classified)

1. ORIGINATING ACTIVITY (Corporate author) HARRY DIAMOND LABORATORIES WASHINGTON, D.C. 20438	2a. REPORT SECURITY CLASSIFICATION UNCLASSIFIED 2b. GROUP

3. REPORT TITLE
FACTORS IN THE DESIGN OF POROUS ELECTRODES FOR PRIMARY ELECTROCHEMICAL CELLS

4. DESCRIPTIVE NOTES (Type of report and inclusive dates)

5. AUTHOR(S) (First name, middle initial, last name)
L. G. Austin and E. G. Gagnon

6. REPORT DATE	7a. TOTAL NO. OF PAGES	7b. NO. OF REFS
May 1969	40	19

8a. CONTRACT OR GRANT NO.	9a. ORIGINATOR'S REPORT NUMBER(S)
b. PROJECT NO. DA-1T061102A34A	Report No. 3
c. AMCMS Code: 5011.11.86000	9b. OTHER REPORT NO(S) (Any other numbers that may be assigned this report)
d. HDL Proj: 96800	

10. DISTRIBUTION STATEMENT
This document has been approved for public release and sale; its distribution is unlimited.

11. SUPPLEMENTARY NOTES	12. SPONSORING MILITARY ACTIVITY
	U. S. Army Materiel Command

13 ABSTRACT

The purpose of this work was to apply the theories of porous electrode behavior to thin, porous electrodes used at low ambient temperatures, to show how performance is affected by the relevant factors involved. The system chosen for study was the Ag-Ag_2O electrode operating in the low-freezing eutectic of aqueous KOH as electrolyte. The report describes the complexity of the cathodic discharge curve; voltage varied with discharge time in six distinct regions. One of these regions, a plateau of almost constant potential was studied in detail. The current density-voltage-temperature relations for this region followed a Tafel equation, with an activation energy of exchange current of 14.5 kcal/mole. For this system an analytical solution was obtained for the equation of behavior. Results from this solution agreed reasonably well with experimental results. In addition, the theory was used to predict the distribution of reaction throughout the electrode and experimental results agreed well with predicted. It is shown how the theory can be used to predict optimum electrode thickness, and how porosity, internal area, and electrolyte conductivity affect the result.

DD FORM 1 NOV 1473 REPLACES DD FORM 1473, 1 JAN 64, WHICH IS OBSOLETE FOR ARMY USE.

UNCLASSIFIED
Security Classification

14. KEY WORDS	LINK A		LINK B		LINK C	
	ROLE	WT	ROLE	WT	ROLE	WT
Porous electrodes	8	3				
Electrode design	8	3				
Silver I Oxide	8	3				